Hetrick, W.A., P.M. Rich, F.J. Barnes, and S.B. Weiss. 1993. GIS-based solar radiation flux models. American Society for Photogrammetry and Remote Sensing Technical Papers. Vol 3, GIS. Photogrammetry, and Modeling. pp 132-143.

GIS-BASED SOLAR RADIATION FLUX MODELS

by

W.A. Hetrick
Department of Electrical and Computer Engineering
University of Kansas
Lawrence, KS 66045

Paul M. Rich
Biological Sciences
University of Kansas
Lawrence, KS 66045

Fairley J. Barnes
Environmental Science Group Mallstop J495, EES-15
Los Alamos, NM 87545

Stuart B. Weiss
Center for Conservation Biology Stanford University
Stanford, CA 94305

ABSTRACT

Solar radiation flux governs such critical ecological processes as heat and gas exchange, primary productivity, and rates of nutrient cycling. We have developed a GIS-based (ARC/INFO) solar radiation flux model (SOLARFLUX) based on surface orientation, seasonal and daily shifts in solar angle, shadows caused by topographic features, and variation in atmospheric conditions. Insolation for any spatial location is calculated by integrating direct and diffuse radiation components over the hemisphere of sky directions for a specified Lime period. Atmospheric conditions can be specified using either empirical or theoretical functions. Insolation can be calculated for any complex surface across a broad range of spatial scales, e.g., locally along the surface of plant canopies or more broadly across the landscape. For natural reserves in both temperate and tropical latitudes--the Big Creek Reserve in California and La Amistad Biosphere Reserve in Costa Rica--SOLARFLUX is being used to study microclimate heterogeneity as it determines habitat quality and thereby influences biodiversity.

INTRODUCTION

Solar radiation is the primary energy source on the surface of the earth, and has pervasive effects on ecosystem structure and function. For example, net radiation sets an upper bound on latent and sensible heat exchange, and therefore limits many ecological processes in conjunction with water supply. Indeed, the major term in energy balance calculations is incident shortwave radiation.

The temporal and spatial distribution of insolation is variable at all scales, but is understandable and subject to quantitative modeling. Temporal variation in global insolation is a function of time of year and cloud cover, and drives seasonal cycles (Lieth 1973). Because global insolation is poorly sampled in weather station networks, models that estimate global insolation and the ratio of direct and diffuse components from standard weather data have been developed (Nicks and Harp 1980, Bristow and Campbell 1984, 1985, Becker and Weingarten 1991). Spatial variation in site-specific insolation at a landscape level is predictable from basic geometric principles, and is a major cause of climatic differentiation across local topography (Geiger 1965). Clear sky insolation across landscapes is a function of latitude, day of year, slope and aspect of the receiving surface, and horizon obstruction. Importantly, these geometric relationships do not change in ecological time. Numerous algorithms and computer programs exist for such calculations (e.g. Swift and Knoerr 1973; Lunde 1980; Nunez 1980; Revfeim 1982)

Integration of spatio-temporal insolation models into a geographical information system (GIS) based model will provide powerful analytical tools for numerous disciplines, from ecology and hydrology to architecture and urban planning. Between-slope differentiation in insolation and its effect on vegetation has been extensively studied in temperate and subarctic latitudes (Shreve 1924; Cottle 1932; Boyko 1947; Cantlon 1953; Nash 1963; Whittaker 1967; Lee and Sypolt 1974; Pahlsson 1974; Armester and Martinez 1978; Gray 1979; Roise and Betters 1981; Westman 1981; Vankat 1982; Tajchman and Wiant 1983; Hicks *et al.* 1984; Running 1984; Holland and Steyn 1985, Segal *et al.* 1985; Edwards and Armbruster 1989; Evans and Young 1989; Lipscomb and Nilsen 1990; among others). On a fine-scale, insolation calculations across hillslopes may be effectively used for population assessment and modeling (e.g. Murphy and Weiss 1988, Weiss *et al.* 1988). Quantification of microclimate at many scales can provide the key to conservation planning at the species level (Murphy *et al.* 1990, Rich and Weiss 1991, Weiss *et al.* 1991), as well as at the community, landscape, and ecosystem level (Mackey *et al.* 1987, Running *et al.* 1987, Murphy and Weiss 1992, Rich *et al.* 1992).

SOLARFLUX is a GIS-based program for modeling solar radiation interception based on surface orientation, solar angle, shadowing due to topographic features, and atmospheric attenuation. Surface topography is defined in a raster-based array (grid) of elevation data. Global location of the surface (longitude and latitude) and time interval for calculation are specified by the user. The result is a grid of total insolation for each surface location during the specified time interval.

METHODS

Programming Approach

SOLARFLUX was developed using ARC/INFO version 6.1 (vector-based) and GRID (raster-based) GIS software (Environmental Systems Research Institute) on a UNIX workstation (SUN SPARCstation 2). The program is written in Arc Macro Language (AML), a programming environment available through the ARC/INFO interpreter. The SOLARFLUX AML makes use of the powerful analysis capabilities of GRID map algebra. Algorithm development for the program was based on a top- down design philosophy, which involved decomposing the complex problem by partitioning it into a series of more manageable problems. Each sub-problem was designed and tested individually and later assembled in the final program. As a result of the design process, a set of modules evolved, each performing a related set of tasks. SOLARFLUX has four categories of modules: 1) the interface module, dedicated to communication with the user, consists of a form menu that prompts the user for the parameters necessary to perform the analysis; 2) the conversion module converts the user defined data into a format acceptable for calculation and performs error checking, for example, converting degrees to decimal degrees and verifying that the value falls in a valid range; 3) the Solar position module calculates the position of the sun, defined by azimuth and zenith angles; and 4) the numerical integration module calculates direct, diffuse, and reflected components of solar radiation. After all of the modules were implemented and tested, an AML driver was written to call each of the modules in turn.

Calculation of Direct insolation

Insolation is calculated by integrating direct, diffuse and reflected radiation components over a specified time interval. Direct radiation is subject to changing solar angle and shading by topographic features (horizon shading). Azimuth and zenith angles of the sun are calculated as a function of day of the year, time, and latitude (Gates 1980):

$$\delta = 23.45(360\,\frac{284+N}{365}) \tag{1}$$

$$\alpha = \arcsin(\cos L\cos\alpha\cos h + \sin L\sin\alpha) \tag{2}$$

$$\alpha = \frac{-\cos\alpha\sin h}{\cos\alpha} \tag{3}$$

$$z = 90-\alpha \tag{4}$$

where α is the solar declination angle, N is Julian day number, α is the solar altitude angle, z is the zenith angle of the sun, α is the solar azimuth angle (zero at North rotating through East), h is the hour angle, and L is the latitude of the surface, all parameters given in degrees.

Direct solar radiation is calculated from the solar constant S_0, the atmospheric transmittance τ, and the angle of incidence between the solar rays and the normal to the plane of interception i (Gates 1980):

$$I_b = S_0\,\tau^m \cos i \tag{5}$$

$$\cos i = \sin\theta\cos a\cos(\alpha - \alpha_s) + \cos\theta\sin a \tag{6}$$

where m is air mass ratio, θ is surface slope angle, a is the elevation angle of the sun, α is the azimuth of the sun, and α_s is the aspect of the surface. In the current version of SOLARFLUX, S_0 is treated as a constant value (1353 W/m^2), though variation caused by the elliptical orbit of earth will be incorporated in future versions.

Atmospheric Effects

A brief consideration of atmospheric effects is important so users of SOLARFLUX can choose reasonable parameter values. The atmosphere is known to be an anisotropic medium, in that the radiation varies with the direction of propagation (Cheng 1989). However, approximations of transmittance are generally isotropic constants. Atmospheric transmittance c accounts for atmospheric attenuation of solar radiation as a direct result of scattering of two forms: 1) Rayleigh scattering due to the molecules of atmospheric gases, and 2) turbidity due to pollution, water vapor, and particulates (Monteith and Unsworth 1990). Because scattering is wavelength dependent, the atmospheric coefficient represents an average scattering over all wavelengths. For most applications of SOLARFLUX, τ is not known, S_0 a reasonable estimate is required of the user. Atmospheric transmittance values range from 0 to 1 and vary with location and elevation. At high elevations with extremely clear air, τ may be as high as 0.8. At lower elevations, on a clear day τ may be 0.7, and a clear sky with high turbidity τ may be as low as 0.4. In the absence of empirical data, Gates (1980) recommends an average value of 0.6 for clear sky conditions.

Atmospheric attenuation is proportional to the air mass through which the radiation must pass. In the early morning and late afternoon attenuation is greater than at solar noon, due to the difference in air mass traversed. The air mass ratio m is the ratio of the path length in the direction of the sun (the zenith angle of the sun with respect to the surface) and the path length in the vertical direction. The ratio varies with the secant of the zenith angle z (Gates 1980):

$$\mathrm{m}=\sec z = \frac{1}{\cos z} \tag{7}$$

Calculation of Diffuse Insolation

SOLARFLUX calculates diffuse solar radiation based on the solar constant S_0, the radiation diffusion coefficient τ_d, the slope of the surface θ, and the elevation angle of the sun a by the following equation (Gates 1980):

$$I_d = S_0\, \tau_d \cos^2 \frac{\theta}{2} \sin a \tag{8}$$

As τ decreases, *i.e.* scattering increases, τ_d increases (Gates 1980):

$$\tau_d = (0.271 - 0.294\tau^m) \tag{9}$$

Calculation of Reflected Insolation

SOLARFLUX calculates reflected solar radiation based on a simple model (Gates1980):

$$I_r = r\, S_0 \sin a\, \tau_r \sin^2 \frac{\theta}{2} \tag{10}$$

where r is the ground reflectance coefficient, S_0 is the solar constant, τ_r is reflectance transmittivity , θ is surface slope, and a is solar elevation angle. Reflectance coefficient r is the mean reflectivity of the surface over a specific spectral band normalized, by the full solar spectrum (Monteith and Unsworth 1990). SOLARFLUX calculates reflectance transmittivity τ_r as a function of τ (Gates 1980):

$$\tau_r = (0.271 - 0.706\tau^m) \tag{11}$$

Calculation of Total Insolation

The total instantaneous insolation is the sum of the direct, diffuse, and reflected radiation components (Gates 1980):

$$\begin{gathered} \mathrm{I} = S_0 \tau^m \cos i + S_0 (0.271 - 0.706\tau^m) \cos^2 \frac{\theta}{2} \sin a + \\ r\, S_0 \sin a\, (0.271 - 0.706\tau^m) \sin^2 \frac{\theta}{2} \end{gathered} \tag{12}$$

where S_0 is the solar constant, τ is atmospheric transmittance coefficient, m is air mass ratio, *i* is the angle of incidence between the normal to the surface and the solar rays, θ is surface slope, *a* is the solar elevation angle, and *r* is the reflected radiation coefficient Solar position is the essential the time dependent component of this expression, so the integration with respect to time is performed by tracing the solar path.

Calculation of Horizon Shading

Horizon shading, blockage of incoming radiation by topography, vegetation, or human-built structures, can be of considerable local importance (Galo *et al.* 1992). Horizon shading primarily affects the direct radiation component at large solar zenith angles (low elevation angles). Direct shading effects depend on solar angle, and therefore must be calculated for each time increment. This is accomplished using the HILLSHADE function in ARC/INFO. This function produces a grid of shadow patterns for a topographic surface, based on solar azimuth and zenith angles. Based on these shadow patterns, SOLARFLUX accounts for blockage of direct radiation at each location along the topographic surface.

Tests of SOLARFLUX

Two surfaces were chosen to interrogate the design and the applicability of SOLARFLUX. The first was a simple surface consisting of 400 grid cells in the shape of a pyramid with a flattened peak and ranging in elevation from 12.5 to 100 units (Figure la). Motivation for using such a surface is two-fold: 1) to serve as a platform for ongoing testing of SOLARFLUX without the excess noise of a complex surface, and 2) to exemplify how SOLARFLUX can be used to simulate local effects of barriers, e.g., a building or tree, on insolation (Figure 2a). The second test surface utilized topographic data for Las Tablas Protected Zone, a region within the La Amistad Biosphere Reserve, Costa Rica (Figure 3a). The surface was generated by manually digitizing topographic contour lines, from which a Triangulated Irregular Network (TIN) model was built and then converted to an elevation grid (Rich *et al.* 1992). This analysis shows how seasonal shifts in solar angle affect insolation at the landscape level for complex surface topography.

RESULTS AND DISCUSSION

The Program

SOLARFLUX uses a form menu that provides a convenient interface for specifying model parameters. The user must supply the input surface grid name, the output grid name, start and end days, start and end times, calculation time increment, global position (latitude and longitude), local time meridian, atmospheric transmittance, and reflectance coefficients. Transmittance can be specified as either a constant or a lookup table that specifies changes with time. Similarly, reflectance can be specified as either a constant or a grid with reflectance properties specified for each location. The output from SOLARFLUX is a grid of total insolation integrated over the specified time interval. Horizon shading can optionally be disabled, allowing assessment of the importance of shadows for different complex surfaces.

Calculations for Test Surfaces

Each slope of the pyramid-shaped theoretical surface receives different insolation depending on its orientation (Figure 1). Figure lb shows the result from running SOLARFLUX for the test surface for a time interval from sunrise to noon on Julian day 260 at 20° N latitude, 10° W longitude. Shading and orientation away from the solar path causes the south slope to have lower values than the north (7.9 vs. 9.9 x 10^6 J/m^2) and the west slope to have lower values (5.8) than the east (5.8 vs. 12.9 x 10^6 J/m^2), while the horizontal slope had a value of 9.8 x 10^6 J/m^2. To demonstrate the impact of shading, a barrier was introduced on the test surface (Figure 2a). This leads to a major reduction of insolation on and below the west face of the barrier.

Las Tablas, on the Pacific slope of the Talamanca Mountains near the Costa Rica Panama border, ranges in elevation from approximately 1,000 to 3,000 m. With a latitude of about 9° N, the solar path ranges from well north of the zenith on the summer solstice and well south on the winter solstice. Consequently total insolation for the summer solstice is much less than the winter solstice (Figure 3).

Applications and Future Development

The current version of SOLARFLUX is a prototype for an increasingly sophisticated GIS-based insolation model. The program is designed with a modular open architecture, which permits modification and enhancement as special needs arise and improved submodels are developed. The user interface allows convenient and complete access to all parameters used in the model. The GIS workstation platform makes it easy to use SOLARFLUX as input to other models, including reflectance models for remote sensing. SOLARFLUX can be readily applied at either local or landscape scales. One very promising application at local scales is study of solar radiation flux in plant canopies, where canopy surface topography leads to heterogeneity in flux processes involving carbon, heat, and water. For example, in pinyon-juniper woodlands, variation in near-ground solar radiation flux, associated with clumped tree distributions, has a strong influence on water balance (Lin *et al.* 1992). At the landscape level, topographic effects on insolation can define the range of microclimates that serve as the physical determinants of habitat for biological organisms (Rich *et al.* 1992). For example, topographic heterogeneity of the Big Creek Reserve, California, leads to a distribution of biotic assemblages that can be predicted on the basis of effects of insolation on microclimate (Saving *et al.* 1993).

Two basic extensions of SOLARFLUX are desirable. First, improved atmospheric transmittivity and diffusion submodels, tailored to describe conditions as they change with time and space, could be implemented as user-specifiable mathematical expressions or lookup tables. Weather conditions and air quality change dramatically over time, and many conditions occur in predictable patterns. For example, clouds may form predictably above mountain ranges, leading to decreased transmittivity and increased diffusion in sky directions toward the mountains. Similarly, transmittivity and diffusion may change predictably through the day as the result of photochemical pollutants.

Second, improved reflectance models, which calculate how surrounding topography affects reflected insolation, can be implemented using viewsheds in an approach similar to that used for horizon shading. Viewshed functions available in GRID permit determination of the direction to surrounding surfaces. Moreover, view position can be specified both on and above the surface, permitting simulations that are likely to give new insights into remote sensing of reflectance patterns (Goel 1988).

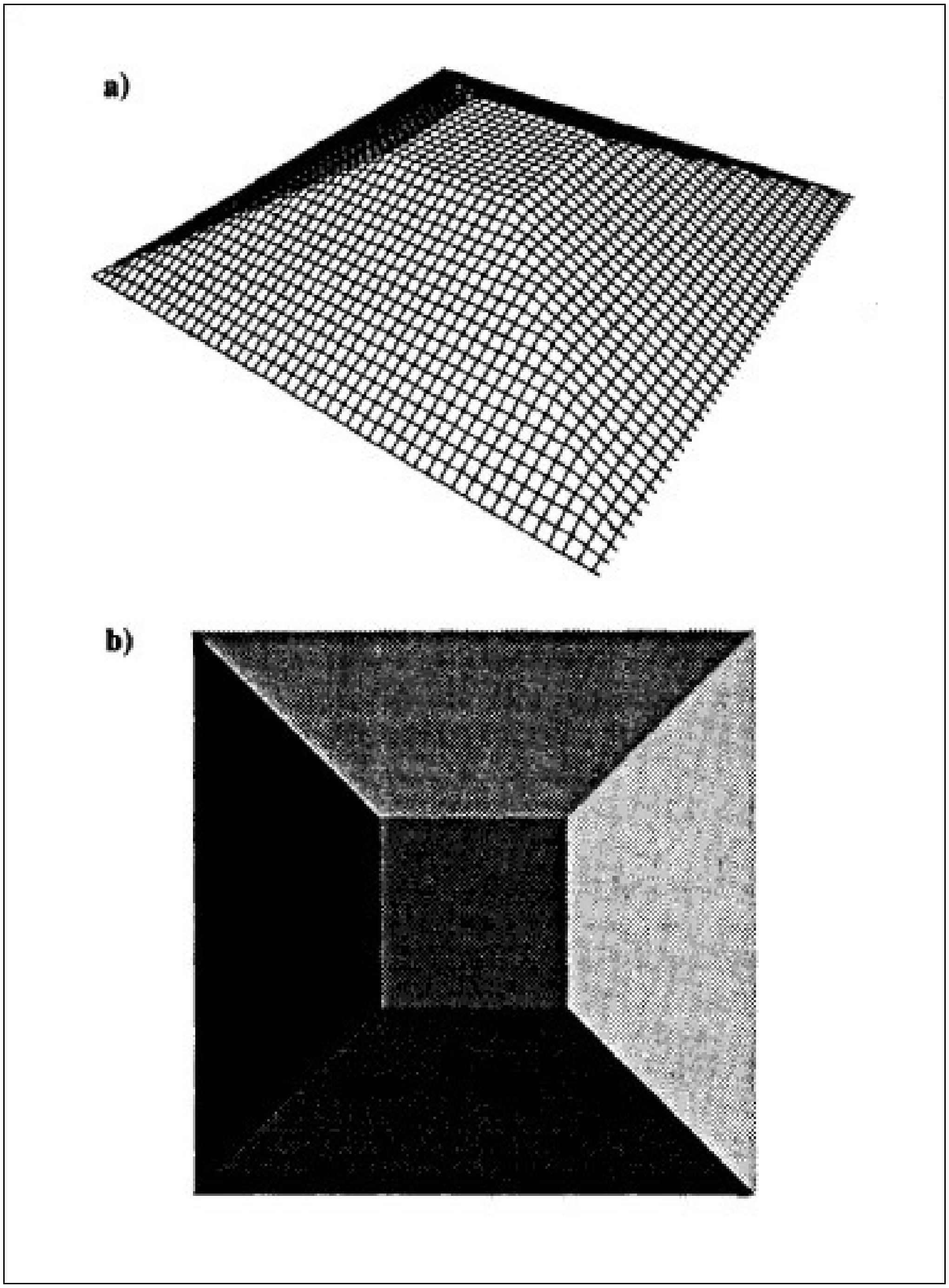

Figure 1 a) View of the theoretical test surface. b) Total insolation for a half-day interval.

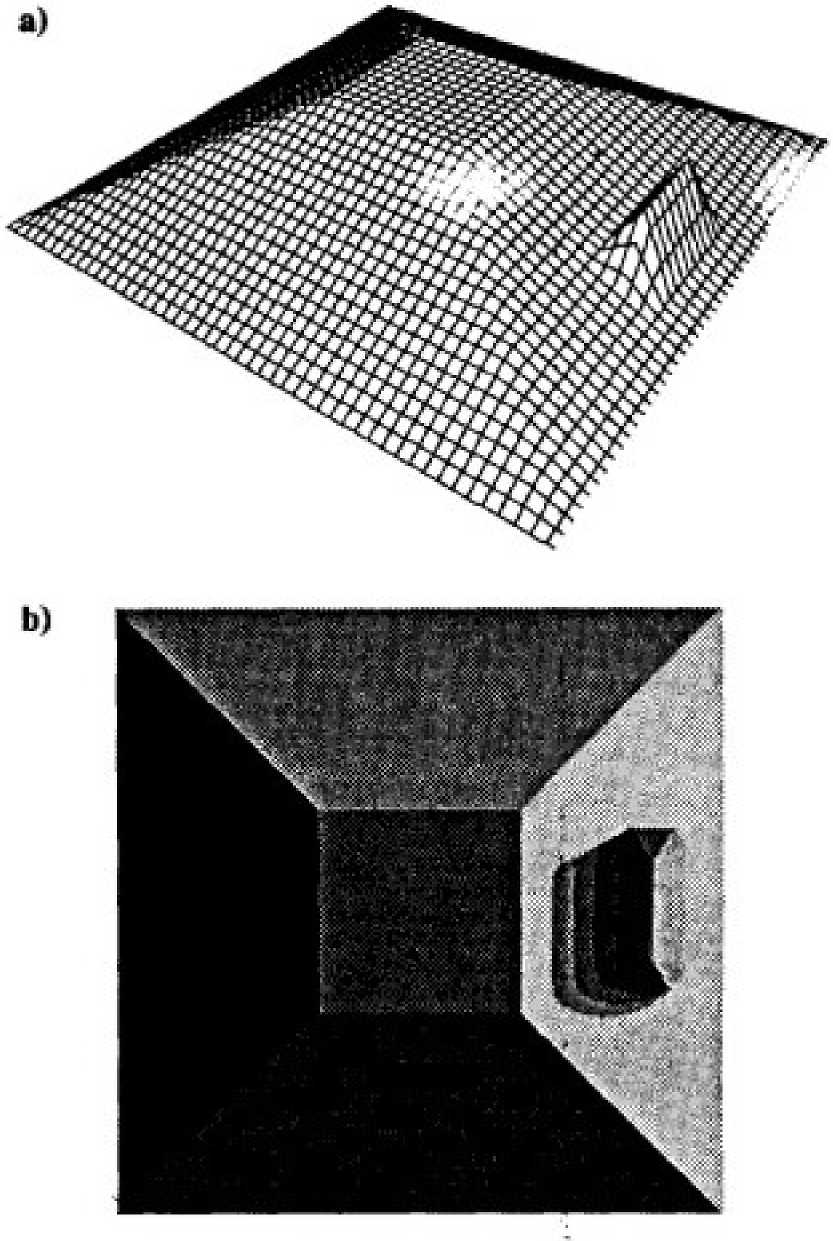

Figure 2 a) View of the theoretical surface with an added barrier. b) Total insolation for a half-day interval.

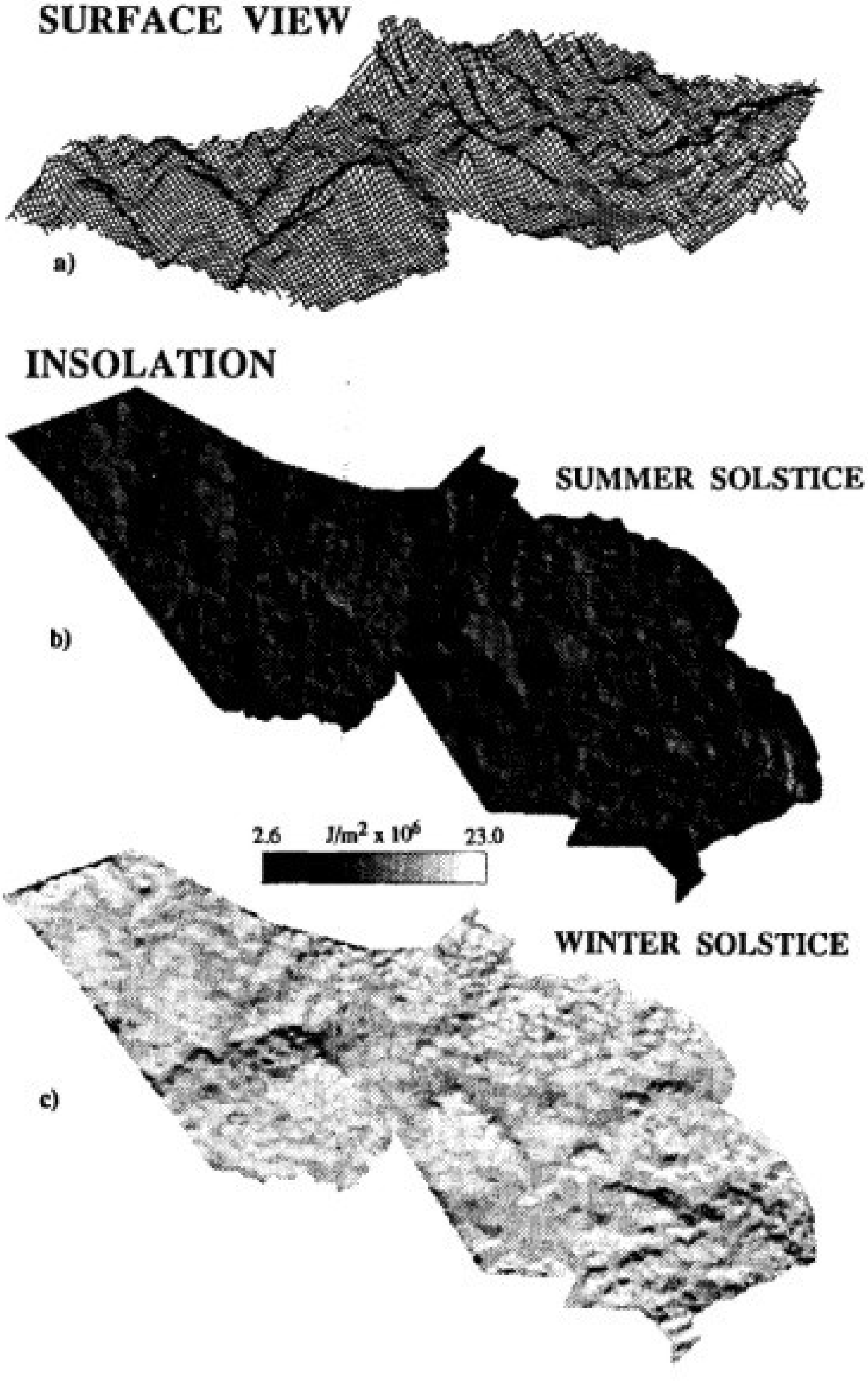

Figure 3 Maps of a) three-dimensional surface topography for Las Tablas Protected Zone, Costa Rica; and theoretical distribution of daily clear-sky insolation for Las Tablas on b) the summer solstice c) the winter solstice.

CONCLUSION

SOLARFLUX is a GIS-based model for calculating insolation for complex surfaces based on surface orientation, solar angle, horizon shading, and atmospheric conditions. This GIS-based approach allows integration of data over surfaces at both local and landscape scales and can readily be coupled to earth system models, with applications in ecology, meteorology, and remote sensing. Computer technology, both software and hardware, now permits us to perform computationally-intensive calculations of how surrounding features influence local conditions, in our case the effect of surrounding topography on insolation.

ACKNOWLEDGEMENTS

This research was supported by National Science Foundation Grant BSR90-02326, a Stanford Center for Conservation Biology grant from the MacArthur Foundation, a University of Kansas General Research Fund Grant, the Los Alamos National Laboratory Environmental Restoration Program (under Department of Energy Contract W-7405-ENG-36), the Kansas Applied Remote Sensing Program, and the Kansas Biological Survey. Additional support was provided by Calcomp Inc., Environmental Systems Research Institute Inc., and SUN Microsystems Inc. We would like to give special thanks to Donna Hetrick, Greg Hughes, Shawn Saving, and Ruby.

REFERENCES

Armester, J.J. and J.A. Martinez. 1978. Relation between vegetation structure and slope aspect in the Mediterranean region of Chile. Journal of Ecology 66: 88 1-889.

Becker, P. and D.S. Weingarten. 1991. A comparison of several models for separating direct and diffuse components of solar radiation. Agricultural and Forest Meteorology 53: 347-353.

Boyko, H. 1947. On the role of plants as quantitative climate indicators and the geoecological law of distribution. Journal of Ecology 35: 138-157.

Bristow, K.L. and G.S. Campbell. 1984. On the relationship between incoming solar radiation and daily maximum and minimum air temperatures. Agricultural and Forest Meteorology 31: 159-166.

Bristow, K.L. and G.S. Campbell. 1985. An equation for separating daily solar radiation into direct and diffuse components. Agricultural and Forest Meteorology 35: 123-131.

Cantlon, J.E. 1953. Vegetation and microclimates on north and south slopes of Cushentuck Mountain, New Jersey. Ecological Monographs 23: 241-270.

Cheng, D.K. 1989. Field and Wave Electromagnetics. Addison-Wesley. Reading.

Cottle, H.J. 1932. Vegetation on the north and south slopes of mountains in southwest Texas. Ecology 12: 121-134.

Edwards, M.E. and W.S. Armbruster. 1989. A tundra-steppe transition on Kathul Mountain, Alaska, U.S.A. Arctic and Alpine Research 21: 296-304.

Evans, R.A. and J.A. Young. 1989. Characterization and analysis of abiotic factors and their influence on vegetation. pp. 13-27 in L.F. Huenneke and H.A Mooney (eds), Grassland Structure and Function: The California Annual Grassland. Dr. W. Junk Publ. Dordrecht.

Feldhake, C.M. and D.G. Boyer. 1990. Bellani evaporation variation in hill-land pasture. Agricultural and Forest Meteorology 51: 211-222.

Gates, D.M. 1980. Biophysical Ecology. Springer-Verlang. New York.

Galo, A.T., P.M. Rich, and J.J. Ewel. 1992. Effects of forest edges on the solar radiation regime in a series of reconstructed tropical ecosystems. American Society for Photogrammetry and Remote Sensing Technical Papers, Albuquerque, NM. pp 98-108.

Gray, J.T. 1979. The vegetation of two California mountain slopes. Madroño 25:177-185.

Geiger, R.J. 1965. The Climate Near the Ground. Harvard University Press. Cambridge.

Goel, N.S. 1988. Models of vegetation canopy reflectance and their use in estimation of biophysical parameters from reflectance data. Remote Sensing Reviews 4: 1-212.

Hicks, R.R. Jr. and P.S. Frank. 1984. Relationship of aspect to soil nutrients, species importance, and biomass in a forested watershed in West Virginia. For. Ecol. Manag. 8: 281-291.

Holland, P.G. and D.G. Steyn. 1975. Vegetational responses to latitudinal variations in slope angle and aspect. Journal of Biogeography 2: 179-183.

Lee, R. and C.R. Sypolt. 1974. Toward a biophysical evaluation of forest site potential. Forest Science 20: 145-154.

Lieth, H. 1973. Phenology and Seasonality Modeling. Ecological Studies 8. Springer Verlag. New York.

Lin, T., P.M. Rich, D.A. Heisler, and F.J. Barnes. 1992. Influences of canopy geometry on near-ground solar radiation and water balances of pinyon-juniper and ponderosa pine woodlands. American Society for Photogrammetry and Remote Sensing Technical Papers, Albuquerque, NM. pp 285-294.

Lipscomb, M.V. and E.T. Nilsen. 1990. Environmental and physiological factors influencing the natural distribution of evergreen and deciduous Ericaceous shrubs on northeast and southwest slopes of the southern Appalachian Mountains. I. irradiation tolerance. American Journal of Botany 77: 108-115.

Lunde, P.J. 1980. Solar Thermal Engineering. John Wiley and Sons: New York.

Mackey, B.G., H.A. Nix, M.F. Hutchinson, J.P. MacMahon, and P.M. Fleming. 1988. Assessing representativeness of places for conservation reservations and heritage listing. Environ. Manag. 12: 501-514.

Monteith J.L. and M.H. Unsworth. 1990. Principles of Environmental Physics. Edward Arnold: London.

Murphy, D.D. and S.B. Weiss. 1988. A long-term monitoring plan for a threatened butterfly. Conservation Biology 2: 367-374.

Murphy, D.D., K.E. Freas, and S.B. Weiss. 1990. An environment-metapopulation approach to population viability analysis for a threatened invertebrate. Conservation Biology 4: 41-51.

Murphy, D.D and S.B. Weiss. 1992. The effects of climate change on biological diversity in western North America: species losses and mechanisms. pp. 355-368 in R. Peters and T. Lovejoy (ads) Global Warming and Biodiversity. Yale University Press. New Haven.

Nash, A.J. 1963. A method for estimating the effects of topography on the soil water balance. Forest Science 9: 413-422.

Nicks, A.D. and J.F. Harp. 1980. The stochastic generation of temperature and solar radiation data. Journal of Hydrology 48: 1-17.

Nunez, M. 1980. The calculation of solar and net radiation in mountainous terrain. Journal of Biogeography 7: 173-186.

Pahlsson, L. 1974. Relationship of soil, microclimate and vegetation on a sandy hill. Oikos 25: 21-34.

Perring, F. 1959. Topographical gradients in chalk grassland. Journal of Ecology. 48:447-481.

Revfeim, K.J.A. 1982. Estimating global radiation on sloping surfaces. New Zealand Journal of Agricultural Research 25: 281-283.

Rich, P.M., S.B. Weiss, D.A. Debinski, and J.F. McLoughlin. 1992. Physiographic inventory of a tropical reserve. Proceedings of the Twelfth Annual ESRI User Conference, Palm Springs, CA. pp 197-208.

Rich, P.M. and SB. Weiss. 1991. Spatial models of microclimate and habitat suitability: lessons from threatened species. pp. 95-102 in Proceedings of the Eleventh Annual ESRI User's Conference. ESRI, Inc: Redlands.

Rich, P.M. 1990. Characterizing plant canopies with hemispherical photography. In: N.S. Goel and J.M. Norman (ads). Instrumentation for studying vegetation canopies for remote sensing in optical and thermal infrared regions. Remote Sensing Reviews 5:13-29.

Roise, J.P. and D.R. Betters. 1981. An aspect transformation with regard to elevation for site productivity models. Forest Science 27: 483-486.

Running, S.W. 1984. Microclimate control of forest productivity: analysis by computer simulation of annual photosynthesis/transpiration balance in different environments. Agricultural and Forest Meteorology 32: 267-288.

Running, S.W., R.R. Nemani, and R.D. Hungerford. 1987. Extrapolation of synoptic meteorological data in mountainous terrain and its use for simulating forest evapotranspiration and photosynthesis. Canadian Journal of Forestry Research 17:472-483.

Saving, S.C., P.M. Rich, J.T. Smiley, and S.B. Weiss. 1993. GIS-based microclimate models for assessment of habitat quality in natural reserves. American Society for Photogrammetry and Remote Sensing Technical Papers, New Orleans, LA. In Press.

Segal, M., Y. Mahrer, R.A. Pileke, and Y. Ookouchi. 1985. Modeling transpiration patterns of vegetation along south and north facing slopes during the subtropical dry season. Agricultural Forest Meteorology 36: 19-28.

Shreve, F. 1924. Influence of slope aspect on soil temperature. Carnegie Institution Yearbook 23: 140-141.

Swift, L.W and K.R. Knoerr. 1973. Estimating solar radiation on mountain slopes. Agricultural Meteorology 12: 329-336.

Tajchman, SJ. and H.V. Wiant Jr. 1983. Topography and biomass characteristics of a forested catchment in the northern Appalachians. For. Ecol. Manag. 5: 55-69.

Tolbert, W.W. 1975. The effects of slope exposure on arthropod distribution patterns. The American Midland Naturalist 94: 38-53.

Vankat, J.L. 1982. A gradient perspective on the vegetation of Sequoia National Park, California. Madroño 29: 200-214.

Weiss, S.B. and D.D. Murphy. 1990. Thermal microenvironments and the restoration of rare butterfly habitat. pp. 50-60 in J. Berger (ed). Environmental Restoration. Island Press. Covelo.

Weiss, S.B., D.D. Murphy, and R.R. White. 1988. Sun, slope, and butterflies: topographic determinants of habitat quality for *Euphydryas editha*. Ecology 69: 1486-1496.

Weiss, S.B., R.R. White, D.D. Murphy, and P.R. Ehrlich. 1987. Growth and dispersal of larvae of the checkerspot butterfly *Euphydryas editha*. Oikos 50: 161-166.

Weiss, S.B., P.M. Rich, D.D. Murphy, W.H. Calved, and P.R. Ehrlich. 1991. Forest canopy structure at overwintering monarch butterfly sites: measurements with hemispherical photography. Conservation Biology 5: 165-175.

Westman, W.E. 1981. Factors influencing the distribution of species of Californian coastal sage scrub. Ecology 62: 439-455.

Whittaker, RH. 1967. Gradient analysis of vegetation. Biological Review 42: 207-264.